

Constrained Bayesian Inference through Posterior Projections

BY S. PATRA

Department of Statistical Science, Duke University, Durham, North Carolina, U.S.A.
sp289@duke.edu

AND D. B. DUNSON

Departments of Statistical Science & Mathematics, Duke University, Durham, North Carolina, U.S.A.
dunson@duke.edu

SUMMARY

In a broad variety of settings, prior information takes the form of parameter restrictions. Bayesian approaches are appealing in parameter constrained problems in allowing a probabilistic characterization of uncertainty in finite samples, while providing a computational machinery for incorporation of complex constraints in hierarchical models. However, the usual Bayesian strategy of directly placing a prior measure on the constrained space, and then conducting posterior computation with Markov chain Monte Carlo algorithms is often intractable. An alternative is to initially conduct computation for an unconstrained or less constrained posterior, and then project draws from this initial posterior to the constrained space through a minimal distance mapping. This approach has been successful in monotone function estimation but has not been considered in broader settings. In this article, we develop a general theory to justify posterior projections in general spaces including for infinite-dimensional functional parameters. For tractability, we initially focus on the case in which the constrained parameter space corresponds to a closed, convex subset of the original space. A special class of non-convex sets called Stiefel manifolds is explored later in the paper. We provide a general formulation of the projected posterior and show that it corresponds to a valid posterior distribution on the constrained space for particular classes of priors and likelihood functions. We also show how asymptotic properties of the unconstrained posterior are transferred to the projected posterior. Posterior projections are then illustrated through multiple examples, both in simulation studies and real data applications.

Some key words: Bayesian; Convexity; Minimal distance mapping; Parameter constraint; Projection operator.

1. INTRODUCTION

Prior information is commonly available in the form of parameter constraints. For example, one may know that the parameters satisfy some set of linear inequalities, that a regression function is monotone in certain directions, or that parameters lie on a probability simplex or manifold. There is a rich literature on statistical methods for incorporating parameter constraints, both from a frequentist and a Bayesian perspective. The Bayesian viewpoint has some advantages in terms of characterizing uncertainty in a probabilistic manner without appealing to large sample size justifications. In addition, asymptotic results can be highly challenging to obtain in parameter constrained problems, and much of the emphasis has been on proving results for special cases. For example, many papers focus specifically on nonparametric estimation subject to monotonicity (Shively et al., 2011) or concavity (Horowitz & Lee, 2017) constraints. However, even though the Bayesian approach to parameter constraints is conceptually broad, posterior

computation is commonly intractable. This has motivated a rich literature on modeling and computational strategies for specific parameter constraints, such as monotonicity in multiple regression functions (Saarela & Arjas, 2011) or Gaussian models subject to linear inequalities (Jidling et al., 2017). There is a clear need for more general approaches.

One intriguing idea that has been proposed in the literature is to initially conduct posterior computation ignoring the parameter constraint, and then project samples from the unconstrained posterior to the constrained space of interest. This posterior projection approach has been specifically developed for ordered parameters (Dunson & Neelon, 2003), unimodality (Gunn & Dunson, 2005) and monotone function estimation (Lin & Dunson, 2014). In such settings, the projected posterior tends to have better performance in several respects than usual Bayesian methods that directly define a posterior on the constrained space. One advantage is computational ease but also the projected posterior tends to reduce bias resulting from parameter constraints. For example, suppose that one wants to estimate a one-dimensional dose response curve characterizing risk of an adverse health response with increasing dose of a chemical exposure. In this setting, it is often reasonable to assume that risk does not decrease with increasing dose, leading to a monotonicity restriction. However, suppose that the sample size is modest and the true dose response curve is close to flat. Usual Bayesian methods, that choose a prior on the space of monotone functions, will tend to badly over-estimate the slope of the dose response curve. The posterior projection approach limits this over-estimation problem by mapping draws from the unconstrained posterior that violate monotonicity to the boundary of the constrained space; this is illustrated by a simpler model in Figure 2.

Although this projected posterior approach is intriguing, it has only been implemented in these specific cases in the previous literature, and the general Bayesian justification for the approach is unclear. The main contribution of this article is to provide a general framework for defining projected posteriors in arbitrary problems, while showing that projected posteriors are valid Bayesian posteriors under some conditions. For tractability theoretically and computationally, we mostly focus on cases in which the constrained space corresponds to a closed, convex subset of the original parameter space. General theory for posterior projection on Stiefel manifolds, a special class of non-convex sets, is developed later in the paper.

2. THEORY & METHODS

2.1. Notation and formulation

Let the data $X^{(n)} = (X_1, \dots, X_n)$ be a random sample following the distribution P_θ , which has a density p_θ with respect to a σ -finite dominating measure on the sample space $(\mathcal{X}^{(n)}, \mathcal{A}^{(n)})$. We assume that the unknown parameter θ belongs to a constrained subset $\tilde{\Theta}$ of the original parameter space Θ , that is $\tilde{\Theta} \subset \Theta$. Usually this restriction is admitted by a prior density $\pi_{\tilde{\Theta}}$ with probability measure $\Pi_{\tilde{\Theta}}$ which is supported on the constrained parameter space $(\tilde{\Theta}, \mathcal{B}_{\tilde{\Theta}})$. Thus the posterior distribution of θ given $X^{(n)}$ is

$$\Pi_{\tilde{\Theta}}(B|X^{(n)}) = \frac{\int_B p_\theta(X^{(n)}) d\Pi_{\tilde{\Theta}}}{\int_{\tilde{\Theta}} p_\theta(X^{(n)}) d\Pi_{\tilde{\Theta}}} \quad \text{for all } B \in \mathcal{B}_{\tilde{\Theta}}. \quad (1)$$

The expression in equation (1) is defined if and only if the denominator is positive. For that it suffices for Θ to be Polish (Ghosal & Van der Vaart, 2017). Assuming $\tilde{\Theta}$ is a non-empty, closed, convex subset of Θ , it is also Polish with its corresponding Borel σ -algebra $\mathcal{B}_{\tilde{\Theta}} = \mathcal{B}_\Theta \cap \tilde{\Theta}$.

A popular choice of restricted prior is $\pi_{\tilde{\Theta}} \propto \pi_\Theta \mathbb{1}_{\tilde{\Theta}}(\theta)$, where π_Θ is an unconstrained probability density on Θ and $\mathbb{1}_{\tilde{\Theta}}(\theta)$ is an indicator function of $\tilde{\Theta}$. Quite often this leads to an intractable posterior which is difficult to sample from. In the case where $\tilde{\Theta}$ has zero measure with respect to the base measure μ_Θ , the posterior in (1) is ill-defined as the denominator is 0.

As an alternative method which avoids these problems, we propose the Posterior Projection approach where initially we ignore the restriction and sample from the unconstrained posterior density $\pi_\Theta(\theta|X^{(n)}) \propto p_\theta(X^{(n)})\pi_\Theta(\theta)$. These samples are then projected to the constrained space $\tilde{\Theta}$ using a minimal distance mapping $T_{\tilde{\Theta}}$. In practice, generating samples from the unconstrained posterior is often

relatively easy and fast. The details about the choice of the minimal distance mapping is discussed in section 2.2.

2.2. Metric projection in general space

In this section we develop the structure of the underlying topological and measure space necessary for the minimal distance mapping. Because Θ is assumed to be Polish, it is also a complete normed vector space $(\Theta, \|\cdot\|)$. We will use the associated metric $\|\cdot\|$ to define the projection operator. For a nonempty subset $\tilde{\Theta}$ of Θ , the distance between the point $\theta \in \Theta$ and the set $\tilde{\Theta}$ is given by the following equation:

$$d(\theta, \tilde{\Theta}) = \inf\{\|\theta - \tilde{\theta}\| : \tilde{\theta} \in \tilde{\Theta}\} \quad (2)$$

A point $\tilde{\theta} \in \tilde{\Theta}$ with $\|\theta - \tilde{\theta}\| = d(\theta, \tilde{\Theta})$ is called a best approximation of θ in $\tilde{\Theta}$.

DEFINITION 1. Let $(\Theta, \|\cdot\|)$ be a complete normed space and $\tilde{\Theta}$ be a nonempty subset of Θ . We define the set valued mapping $T_{\tilde{\Theta}} : \Theta \rightarrow \mathcal{P}(\Theta)$ by

$$T_{\tilde{\Theta}}(\theta) = \{\tilde{\theta} \in \tilde{\Theta} : \|\theta - \tilde{\theta}\| = d(\theta, \tilde{\Theta})\} \quad (3)$$

and refer to it as the metric projection operator onto $\tilde{\Theta}$.

When there is no ambiguity about the constrained space $\tilde{\Theta}$ we omit the subscript and denote $T_{\tilde{\Theta}}(\theta)$ by $T\theta$. Clearly T is idempotent, that is $T \circ T = T$. Additionally if we denote the set inverse of T by $T^{-1}B = \{\theta \in \Theta \mid T\theta \in B\}$, we get

$$A \subseteq T^{-1} \circ TA, \quad B = T \circ T^{-1}B, \quad \text{for all } A \in \mathcal{B}_{\Theta}, B \in \mathcal{B}_{\tilde{\Theta}}.$$

Basic concerns in the metric projection problem include the existence and uniqueness which are dependent on the parameters $(\Theta, d, \tilde{\Theta}, \theta)$. We say $\tilde{\Theta}$ is a proximal set if $T\theta \neq \emptyset$ and that $\tilde{\Theta}$ is a Chebyshev set if $T\theta$ is a singleton for each $\theta \in \Theta$. The proximality condition is vital as it allows one to explicitly compute the post sampling projections while the Chebyshev condition guarantees the uniqueness. We illustrate these concepts with examples in \mathbb{R}^2 ; refer to Fig. 1.

Assume that the constrained space is the closed unit ball $B[0, 1]$ equipped with the Euclidean norm. It is easy to see that any point within the circle gets mapped back to itself while a point outside gets projected radially, that is $T\theta = \theta/\|\theta\|$ for $\theta \notin B[0, 1]$. Here every point has a unique projection and hence $B[0, 1]$ is a Chebyshev set. Now consider that the constrained space is the region outside the open unit ball, that is $\tilde{\Theta} = \mathbb{R}^2 \setminus B(0, 1)$. In this case every element in the boundary of the unit ball is equidistant from the centre 0, therefore $T(0) = S_{\mathbb{R}^2}$, the unit circle. Every other element of $B(0, 1)$ has a unique radial projection as before, hence $\tilde{\Theta}$ is proximal.

When the metric projection T is a measurable mapping between spaces $(\Theta, \mathcal{B}_{\Theta})$ and $(\tilde{\Theta}, \mathcal{B}_{\tilde{\Theta}})$, which is guaranteed by the Assumption 3 introduced later, T induces a pushforward measure $\tilde{\Pi}_{\tilde{\Theta}}(\cdot | X^{(n)})$ on $\tilde{\Theta}$ corresponding to a posterior measure $\Pi_{\Theta}(\cdot | X^{(n)})$ on Θ . For any $B \in \mathcal{B}_{\tilde{\Theta}}$ this is given by

$$\tilde{\Pi}_{\tilde{\Theta}}^{(n)} B = \tilde{\Pi}_{\tilde{\Theta}}(\cdot | X^{(n)})(B) = \Pi_{\Theta}(\cdot | X^{(n)})(T^{-1}B) = \Pi_{\Theta}^{(n)}(T^{-1}B). \quad (4)$$

We refer to $\Pi_{\Theta}(\cdot | X^{(n)})$ and $\tilde{\Pi}_{\tilde{\Theta}}(\cdot | X^{(n)})$ as the original or unrestricted posterior and the constrained or projected posterior and use the shorthand notations $\Pi_{\Theta}^{(n)}$ and $\tilde{\Pi}_{\tilde{\Theta}}^{(n)}$, respectively.

2.3. Existence of prior on the restricted space

Our aim in this section is to establish a Bayesian justification for our posterior projection scheme. We will prove the existence of a prior $\Pi_{\tilde{\Theta}}$ such that the resulting posterior $\Pi_{\tilde{\Theta}}(\cdot | X^{(n)})$ is equivalent to the projected posterior $\tilde{\Pi}_{\tilde{\Theta}}^{(n)}$ almost everywhere. Mathematically, for any $B \in \mathcal{B}_{\tilde{\Theta}}$ we want

$$\tilde{\Pi}_{\tilde{\Theta}}^{(n)} B = \Pi_{\tilde{\Theta}}(B | X^{(n)}).$$

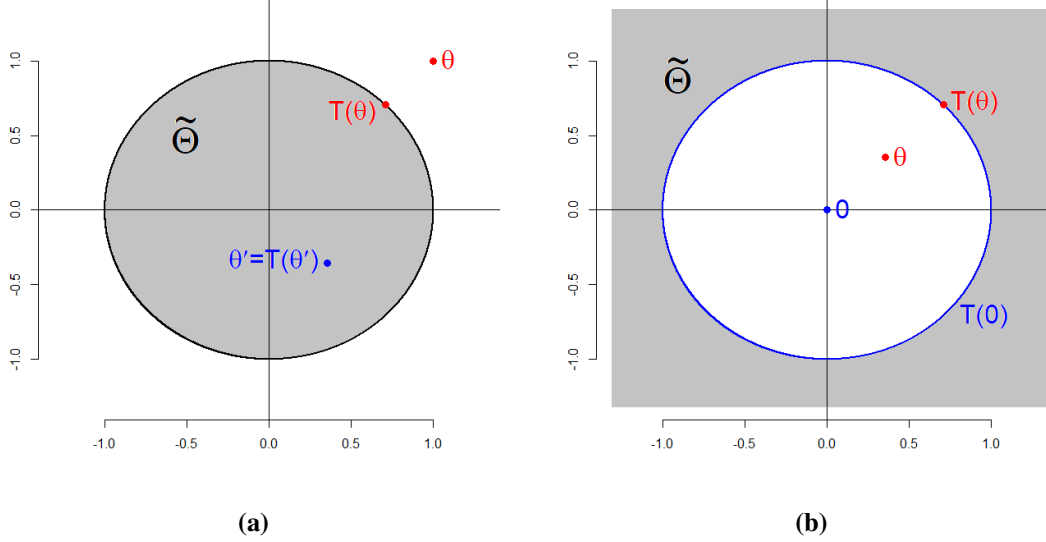


Fig. 1: Illustration of the Metric projection operator T in \mathbb{R}^2 under the Euclidean norm when the constrained space, denoted by the shaded region in the figure, is (a) Chebyshev set and (b) proximal set. A point and its corresponding projection set are indicated by the same color.

This condition is satisfied when the projected posterior has a density $\tilde{\pi}_{\tilde{\Theta}}^{(n)}$ with respect to a σ -finite measure $\mu_{\tilde{\Theta}}$ on $\tilde{\Theta}$ (Theorem 1).

Assumption 1. The projected posterior has a density $\tilde{\pi}_{\tilde{\Theta}}^{(n)}$, given by the Radon-Nikodym derivative with respect to a σ -finite measure $\mu_{\tilde{\Theta}}$ on $\tilde{\Theta}$.

The question of when such a density exists is a tricky one. For example, suppose $X = f(\theta) + \epsilon$, f is constrained to be non-decreasing, and the original prior is $f \sim \text{GP}(0, K)$ corresponding to a Gaussian process with covariance function K . Then one runs into the difficult problem of defining densities on function spaces. We begin to unravel this mystery with the following lemma which will be instrumental in the subsequent arguments.

LEMMA 1. *Let λ_{Θ} and μ_{Θ} be two measures on the original parameter space Θ such that $\lambda_{\Theta} \ll \mu_{\Theta}$. Then the metric projection T preserves absolute continuity, that is $\tilde{\lambda}_{\tilde{\Theta}} \ll \tilde{\mu}_{\tilde{\Theta}}$.*

As an immediate corollary, we notice that when the posterior measure is absolutely continuous with respect to the prior (an exception is non-parametric Dirichlet prior, see Ghosal & Van der Vaart (2017) for more details), the corresponding projected posterior is also absolutely continuous with respect to the projected prior measure. The same logic can be applied for the σ -finite base measure μ_{Θ} to obtain the following result.

$$\Pi_{\Theta}^{(n)} \ll \Pi_{\Theta} \ll \mu_{\Theta} \implies \tilde{\Pi}_{\tilde{\Theta}}^{(n)} \ll \tilde{\Pi}_{\tilde{\Theta}} \ll \tilde{\mu}_{\tilde{\Theta}}$$

We observe that while the projection map preserves absolute continuity (Lemma 1), it does not ensure retention of the σ -finite property. Therefore, even if the unrestricted posterior measure $\Pi_{\Theta}^{(n)}$ had a density with respect to a base measure μ_{Θ} on Θ , there is no guarantee that the projected posterior $\tilde{\Pi}_{\tilde{\Theta}}^{(n)}$ will have a density with respect to the projected base measure $\tilde{\mu}_{\tilde{\Theta}}$. However, one can generally construct a reference

measure in $\tilde{\Theta}$ with respect to which the density exists. One such possibility is using $\tilde{\Pi}_{\tilde{\Theta}}$ as a reference measure when $\Pi_{\tilde{\Theta}}^{(n)} \ll \Pi_{\Theta}$ is true. Because Π_{Θ} is finite, $\tilde{\Pi}_{\tilde{\Theta}}$ is σ -finite, and thus $\Pi_{\tilde{\Theta}}^{(n)}$ has a density (Assumption 1). These ideas are thoroughly discussed with respect to an example in Appendix C of the Supplementary Materials.

THEOREM 1. *Let the unrestricted posterior measure $\Pi_{\Theta}^{(n)}$ induce the constrained posterior measure $\tilde{\Pi}_{\tilde{\Theta}}^{(n)}$ through the metric projection T . Then under Assumption 1 there exists a prior density $\pi_{\tilde{\Theta}}$ on the constrained parameter space such that the corresponding posterior density is equal to the projected posterior density $\tilde{\pi}_{\tilde{\Theta}}^{(n)}$ almost everywhere.*

3. METRIC PROJECTION ONTO CLOSED AND CONVEX SETS

3.1. Convergence properties on closed and convex sets

This section focuses on the frequentist properties of the projected posterior distribution $\tilde{\Pi}_{\tilde{\Theta}}^{(n)}$ as $n \rightarrow \infty$. We study the rate at which the posterior concentrates on arbitrarily small neighbourhoods of $P_{\theta_0}^{(n)}$, where $\theta_0 \in \Theta$ denotes the true value of the parameter. Let the unrestricted posterior $\Pi_{\Theta}^{(n)}(\cdot | X^{(n)})$ have rate ϵ_n with respect to a semimetric d_{Θ} on Θ in the following sense:

$$\Pi_{\Theta}^{(n)}\left(\theta : d_{\Theta}(\theta, \theta_0) > M_n \epsilon_n \mid X^{(n)}\right) \rightarrow 0, \quad \text{for every } M_n \rightarrow \infty, \quad P_{\theta_0}^{(n)}(a.s.). \quad (5)$$

We need to impose further regulatory conditions on the parameter space to ensure posterior consistency. We list the assumptions below and discuss their necessity and implications.

Assumption 2. $(\Theta, \|\cdot\|)$ is a separable, uniformly convex and uniformly smooth Banach space.

We work with Banach spaces as they are a complete normed vector space making calculations more tractable. We also add a separability condition so that Θ is a Polish space which is required for equation (1) to be defined. In corollary 1 we give examples of some familiar spaces where this assumption is realized.

Assumption 3. $\tilde{\Theta}$ is a nonempty, closed, convex subset of Θ .

Milman-Pettis theorem states that every uniformly convex Banach space is reflexive and strictly convex. Therefore the metric projection operator T is continuous and $\tilde{\Theta}$ is a Chebyshev set (Li (2004), Theorem E). More importantly, T has the following local Lipschitz continuity property (Li (2004), Theorem G):

$$\|T\theta - \tilde{\theta}\| \leq \|\theta - \tilde{\theta}\|, \quad \text{for any } \theta \in \Theta \text{ and } \tilde{\theta} \in \tilde{\Theta}.$$

This property is called Lipschitz continuity mod $\tilde{\Theta}$. It is a relaxation of uniform continuity, which is a very strict global condition and difficult to obtain in practice.

Assumption 4. The semimetric d_{Θ} is biLipschitz with respect to $(\Theta, \|\cdot\|)$; that is there exists a constant $C \geq 1$ such that

$$C^{-1} \|\theta - \theta'\| \leq d_{\Theta}(\theta, \theta') \leq C \|\theta - \theta'\|, \quad \text{for any } \theta, \theta' \in \Theta.$$

The implication of this condition becomes evident when considering any norm equivalent to $\|\cdot\|$, specifically all the L_p norms for $p > 0$ in a finite dimensional Euclidean space are equivalent. One might ask why not use d_{Θ} as the underlying distance function of the projection operator in the first place. Firstly d_{Θ} is not guaranteed to be a metric. More importantly, the projection map might be easier to compute with respect to $\|\cdot\|$ than d_{Θ} . For example, in \mathbb{R} the projection operator has a closed form solution with respect to the L_2 norm, but needs to be calculated numerically for L_1 norm.

THEOREM 2. *If the true parameter value $\theta_0 \in \tilde{\Theta}$, then under Assumptions 2-4 the concentration rate of the projected posterior is at least that of the original posterior.*

As an immediate consequence of Theorem 2 we note some of the well-known spaces that satisfy Assumption 2.

COROLLARY 1. *The statement of Theorem 2 is realized in the following spaces.*

1. $\ell_p^n, 1 \leq p \leq \infty$: the space of all n -dimensional sequences with finite p -norm.
2. $\ell_p, 1 < p < \infty$: the space of all countably infinite dimensional sequences with finite p -norm.
3. $L_p(\mu), 1 < p < \infty$: the space of all functions with finite p -norm with respect to the measure μ .

The statement of Theorem 2 can be extended to the case where θ_0 is outside the restricted region $\tilde{\Theta}$ when Θ is a Hilbert space. This is because metric projection onto a closed convex subset of Hilbert space is non expansive (Fitzpatrick & Phelps, 1982), that is

$$\|T\theta - T\theta'\| \leq \|\theta - \theta'\|, \quad \text{for any } \theta, \theta' \in \Theta. \quad (6)$$

Therefore in Hilbert spaces we achieve the following theorem.

THEOREM 3. *Let Θ be a separable Hilbert space. If the original posterior $\Pi_{\Theta}^{(n)}$ converges to θ_0 at the rate ϵ_n , then under Assumptions 2–4 the projected posterior converges to $T\theta_0$ at the rate at least ϵ_n .*

As an immediate corollary we list a few familiar spaces where the statement of the Theorem 3 is valid.

COROLLARY 2. *The statement of Theorem 3 is realized in the following spaces.*

1. \mathbb{C}^n : n -dimensional Euclidean space over complex numbers \mathbb{C} .
2. ℓ_2^n : the space of all n -dimensional square-summable sequences.
3. ℓ_2 : the space of all countably infinite dimensional square-summable sequences.
4. $L_2(\mu)$: the space of square-integrable functions with respect to the measure μ .

3.2. Gaussian projection onto the non-negative real line

As a simple illustrative example we consider a univariate Gaussian likelihood with a conjugate prior. Let $X^{(n)} = (x_1, x_2, \dots, x_n)$ be such that $x_i \sim N(\theta, 1)$, $i = (1, \dots, n)$ and $\theta \geq 0$. In such cases it is common to put a truncated prior on the parameter; for example $\theta \sim N_{(0, \infty)}(0, 1000)$; Here $N_{(0, \infty)}$ denotes the normal distribution truncated onto the nonnegative real line. The posterior of θ is then given by

$$\theta | X^{(n)} \sim N_{(0, \infty)}(\theta_n, \sigma_n^2), \quad \theta_n = \frac{n\bar{x}}{1/1000 + n}, \quad \sigma_n^2 = \frac{1}{1/1000 + n} \quad (7)$$

which is equivalent to sampling from the unconstrained posterior and discarding negative values. This posterior density assigns no probability to the boundary 0 and has expectation

$$E(\theta | X^{(n)}) = \theta_n + \frac{\phi(\alpha)}{1 - \Phi(\alpha)} \sigma_n \quad (8)$$

where $\alpha = -\theta_n/\sigma_n$, ϕ and Φ denote the density and distribution function of the standard normal, respectively.

In the posterior projection approach we initially ignore the constraint on θ , and use the unrestricted prior $\theta \sim N(0, 1000)$. The resulting posterior is $\theta | X^{(n)} \sim N(\theta_n, \sigma_n^2)$ which has the same form as equation (7) but without the truncation. Next we obtain samples θ_s from the unconstrained posterior and set $\tilde{\theta}_s$ to 0 if θ_s is negative, and equal to θ_s otherwise. Thus the projected posterior on $[0, \infty)$ has the following density:

$$\tilde{\pi}_{[0, \infty)}^{(n)}(\tilde{\theta}) = \Phi(\alpha) \mathbb{1}_0(\tilde{\theta}) + [1 - \Phi(\alpha)] N_{(0, \infty)}(\tilde{\theta}; \theta_n, \sigma_n^2) \quad (9)$$

Here $\mathbb{1}_0(\tilde{\theta})$ is the indicator of whether $\tilde{\theta}$ is 0 or not. This posterior density (9) has expectation

$$E(\tilde{\theta} | X^{(n)}) = [1 - \Phi(\alpha)] \left(\theta_n + \frac{\phi(\alpha)}{1 - \Phi(\alpha)} \sigma_n \right)$$

which is closer to θ_n than the expression in (8). The incorporation of the constraint reduces the uncertainty in the posterior distribution, and projecting the draws that violate the constraint to the boundary allocates higher posterior probability to values that are close to θ_n . This property is appealing since θ_n is a function of \bar{x} , which is an unbiased and consistent estimator of θ .

To explore the effect of the projection technique we simulate $n = 25$ datapoints from $N(\theta_0, 1)$ where the value of θ_0 is fixed at $-0.5, 0$ and 0.5 , respectively. These cases correspond to being outside, at the boundary and inside the constrained parameter space. For each sample the unconstrained, truncated and projected posterior densities and posterior mean are plotted in Fig. 2. When the data are in conflict with the constraint ($\theta_0 = -0.5$) the difference in the approaches is very prominent. Even when the data agree with the constraint, but the truth is at the boundary ($\theta_0 = 0$), the posterior mean of the projection approach is closer to the θ_0 than that of the truncated posterior. The posterior densities coincides when the true value is well inside the constrained region.

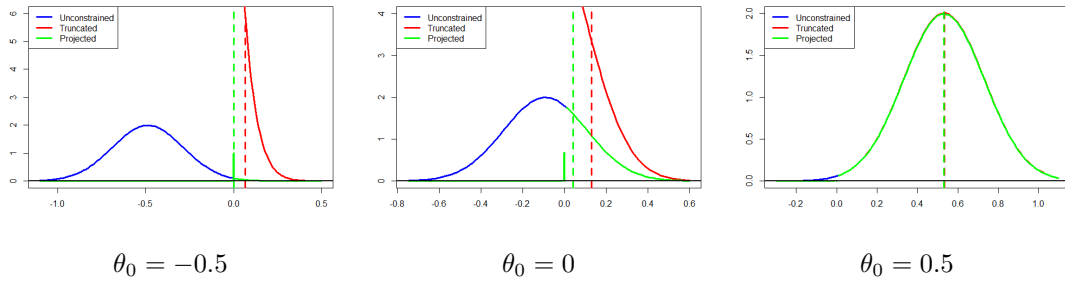


Fig. 2: Illustration of the effect of the projection technique when the true parameter value θ_0 is outside, at the boundary and inside of the constrained parameter space. In each panel the solid lines represent posterior densities for the Gaussian mean under a noninformative unconstrained $N(0, 1000)$ prior (blue), corresponding projection approach (green) and the truncated $N_{(0, \infty)}(0, 1000)$ prior (blue). The associated posterior means, represented by the dotted vertical lines, are closer to the true parameter value than the truncated one.

It is also possible to determine the prior on the non-negative real line which leads to the projected posterior density in (9). This prior density is given by

$$\pi_{[0, \infty)}(\tilde{\theta}) = w_1 \mathbb{1}_0(\tilde{\theta}) + w_2 N_{(0, \infty)}(\tilde{\theta}; \theta_0, \sigma_0^2)$$

where $w_j = (W_j^0/C_j)/(\sum_{j=1}^2 W_j^0/C_j)$, W_j^0 denotes the corresponding weights in the expression (9) and C_j 's are given by

$$C_1 = N(0; \bar{x}, 1/n), \quad C_2 = N(0; \bar{x}, 1/n) \frac{N_{(0, \infty)}(0; 0, 1000)}{N_{(0, \infty)}(0; \theta_n, \sigma_n^2)}.$$

Details of the derivation for a non standard Gaussian is provided in the Appendix C of the Supplementary Materials. It is important to note that the $\pi_{[0, \infty)}(\tilde{\theta})$ is heavily data dependent and this is true in general for the posterior projection approach.

4. METRIC PROJECTION ONTO STIEFEL MANIFOLDS

4.1. Background and notation

The Stiefel manifold is an important space which arises naturally in modeling of subspaces and in applications such as human activity modelling (Veeraraghavan et al., 2005), video based face recognition (Aggarwal et al., 2004), and shape analysis (Goodall & Mardia, 1999). Edelman et al. (1998) give a

detailed overview of the well studied geometric properties of this manifold. For our purpose, we restrict our attention to finite dimensional Stiefel manifolds on \mathbb{R}^m .

DEFINITION 2. *Let $p, m \in \mathbb{N}, 1 \leq p \leq m$. Then the Stiefel manifold $St(p, m) = \tilde{\Theta}$ is the subset of $\mathbb{R}^{m \times p} = \Theta$ consisting of all orthonormal p -frames. Mathematically,*

$$St(p, m) = \{\theta \in \mathbb{R}^{m \times p} \mid \theta^T \theta = I_p\}. \quad (10)$$

For example, when $p = m$, $St(m, m)$ coincides with $O(m)$, the set of all real orthonormal matrices of size m . When $p = 1$, $St(1, m) = \mathbb{S}^{m-1}$, the $m - 1$ dimensional manifold of unit circle in \mathbb{R}^m . It follows that $St(p, m)$ is a closed subspace of the p -fold Cartesian product of \mathbb{S}^{m-1} as $St(p, m)$ is given by p unit vectors $\theta_1, \dots, \theta_p \in \mathbb{R}^m$ such that $\langle \theta_i, \theta_j \rangle = 0$ for all $i \neq j$.

4.2. Properties of the projection

It is evident from the definition 2 that $St(p, m)$ is not a convex set. However, the Stiefel manifold is a smooth embedded closed submanifold of $\mathbb{R}^{m \times p}$, which itself is a Hilbert space endowed with the inner product $\langle \theta_1, \theta_2 \rangle = \text{trace}(\theta_1^T \theta_2)$. Therefore one may define a probability on $\mathbb{R}^{m \times p}$ and project it to $St(p, m)$. The following result ensures the validity of this technique.

LEMMA 2. *For almost every $\theta \in \mathbb{R}^{m \times p}$ there exists a unique projection $T\theta \in St(p, m)$.*

The implication of this proposition is that for any posterior measure $\Pi_{\Theta}^{(n)}$ that is locally absolutely continuous with respect to Lebesgue measure on $\mathbb{R}^{m \times p}$, the projected posterior measure $\tilde{\Pi}_{\tilde{\Theta}}^{(n)}$ is well defined on $St(p, m)$. It is also possible to characterize the set for which the projection is unique.

LEMMA 3. *Only the set of matrices with full column rank p , denoted Θ_p , has unique projection on $St(p, m)$.*

$$\Theta_p = \{\theta \in \mathbb{R}^{m \times p} \mid \text{rank}(\theta) = p\}. \quad (11)$$

This follows immediately from Bardelli & Mennucci (2017), proposition 4.8. This result depicts the importance of choosing a lower value of p , if possible, while modeling using the posterior projection method because the dimension of Θ_p , given by mp , grows linearly with p . Intuitively it becomes harder to find p independent vectors in \mathbb{R}^m as p grows larger. Trivially $St(p, m) \subset \Theta_p$.

PROPOSITION 1. *Θ_p is an open set containing $St(p, m)$.*

Because Θ_p is an open set every matrix close to a matrix in the Stiefel manifold has full rank. Specifically, if $\|\theta - \tilde{\theta}\| < 1$, for some $\tilde{\theta} \in St(p, m)$ then θ has rank p (Absil & Malick, 2012). Thus if our posterior converges to a point on the Stiefel manifold every point in the vicinity is guaranteed to have a unique projection.

As we noted earlier, $St(p, m)$ is not convex. Therefore we are going to focus on its convex hull, which is defined as the smallest convex set of the vector space $\mathbb{R}^{m \times p}$ that contains $St(p, m)$ and is denoted as $\text{conv}(St(p, m))$. The closed convex hull is the closure of its convex hull.

THEOREM 4 (JOURNE ET AL. (2010)). *The convex hull of the Stiefel manifold is the closed unit spectral ball.*

The unit spectral ball is given by

$$\mathbb{B}_{\text{Sp}}(p, m) = \{\theta \in \mathbb{R}^{m \times p} : \|\theta\|_2 \leq 1\} = \{\theta \in \mathbb{R}^{m \times p} : \theta^T \theta \preceq I_p\}, \quad (12)$$

where the spectral norm $\|\theta\|_2$ is the largest singular value of the matrix θ . The boundary of the spectral ball is given by all matrices with largest singular value equal to 1. Because any element of $St(p, m)$ has exactly p singular values all of which are equal to 1, the Stiefel manifold is a subset of the boundary of its convex hull. Interestingly, it is also the subset of the boundary of $\mathbb{B}_{\sqrt{p}}$, the closed centered ball of matrices in $\mathbb{R}^{m \times p}$ with Frobenius norm less than or equal to $p^{1/2}$. When $p = 1$, these two balls coincide. This is

important as the metric projection onto $\text{St}(p, m)$ tries to minimize the Frobenius norm, for any $\theta \in \Theta$,

$$T\theta = \arg \min_{\tilde{\theta} \in \text{St}(p, m)} \|\theta - \tilde{\theta}\|^2 = \arg \max_{\tilde{\theta} \in \text{St}(p, m)} \text{trace}(\theta^T \tilde{\theta}).$$

From this equivalent representation one can obtain a closed form solution for the projection which ties the spectral and Frobenius ball.

PROPOSITION 2. *Let UDV^T be a thin singular value decomposition (SVD) of $\theta \in \Theta_p$, that is U is a $m \times p$ matrix. Then the projection is given by $T\theta = UV^T$.*

A proof of this proposition can be found in Absil & Malick (2012), proposition 7. An immediate consequence of the result is that the projection is unaltered by a change in scale. This is because for a non-negative constant $c > 0$, a thin SVD of $c\theta$ is given by $U(cD)V^T$. In particular $\theta/\|\theta\|_2$ has the same projection as θ and belongs to $\mathbb{B}_{\text{sp}}(p, m)$ as its maximum eigenvalue is 1. We will use this trick to scale our samples of U prior to projection in the brain analysis example (section 5.2) for better estimation and prediction.

4.3. Convergence on Stiefel manifold

Even though Θ is a Hilbert space in this case, the projection operator T on $\text{St}(p, m)$ is not non-expansive. This property was a key component of establishing posterior consistency in a convex subset $\tilde{\Theta}$ of a Hilbert space Θ (section 3.1). Let us consider the following example.

Example 1. Consider three matrices in $\mathbb{R}^{2 \times 2}$

$$\theta_1 = \begin{bmatrix} 1 & 0 \\ 0 & 1 \end{bmatrix}, \quad \theta_2 = \begin{bmatrix} 0 & 1 \\ 1 & 0 \end{bmatrix}, \quad \text{and} \quad \theta_3 = \begin{bmatrix} 0.25 & 0.75 \\ 0.75 & 0.25 \end{bmatrix}$$

It is easy to see that $\theta_1, \theta_2 \in \text{St}(2, 2)$. The matrix θ_3 has singular values 1 and 0.5 and therefore does not belong to $\text{St}(2, 2)$. In fact $T\theta_3 = \theta_2$ which satisfies the following inequality.

$$\|T\theta_3 - T\theta_1\| = \|\theta_2 - \theta_1\| = 2 > 1.5 = \|\theta_3 - \theta_1\|.$$

Therefore, T is not non expansive.

However, we can use the triangle inequality to establish that T is Lipschitz continuous mod $\text{St}(p, m)$.

LEMMA 4. $\|T\theta - \tilde{\theta}\| \leq 2 \|\theta - \tilde{\theta}\|$ for any $\theta \in \mathbb{R}^{m \times p}$, $\tilde{\theta} \in \text{St}(p, m)$.

Coupled with Lemma 2 and 3 this gives us our desired consistency result. Interestingly, even when θ does not have a unique projection, Lemma 4 holds for every element of $T\theta$. Therefore, for convergence purposes any projection of $\theta \notin \Theta_p$ suffices.

THEOREM 5. *If the true matrix $\theta_0 \in \text{St}(p, m)$, then under Assumption 4 the concentration rate of the projected posterior is at least that of the original posterior.*

4.4. Metric projection onto measure 0 sets

It is clear from Fig. 1 that the metric projection T maps elements outside the constrained region to the boundary. One might wonder what happens when the constrained parameter space has measure 0, so that $\Pi_{\tilde{\Theta}}^{(n)} \tilde{\Theta} = 0$. However, our object of interest is the projected posterior under which the constrained space has measure 1, as $\tilde{\Pi}_{\tilde{\Theta}}^{(n)} \tilde{\Theta} = \Pi_{\Theta}^{(n)} \Theta = 1$. This argument extends to any subset $B \in \tilde{\Theta}$, that is even if $\Pi_{\tilde{\Theta}}^{(n)} B = 0$, $\tilde{\Pi}_{\tilde{\Theta}}^{(n)} B \geq 0$. Therefore it is of clear importance to properly identify the underlying probability measure. We illustrate this via modeling on $\text{St}(1, m)$, the $(m - 1)$ dimensional unit sphere $\tilde{\Theta} = \mathbb{S}^{m-1}$ on $\Theta = \mathbb{R}^m$, with $m = 3$. Let

$$x_i \sim N(\theta, 10I), i = (1, \dots, 100), \quad \theta \sim \text{VMF}(\mu, \phi^{-1}I),$$

where $\text{VMF}(\mu, \phi^{-1}I)$ is the von Mises-Fisher distribution with $\mu, \theta \in \tilde{\Theta}$. The resulting posterior is $\text{VMF}(\mu_n, \phi_n^{-1}I)$ where

$$\phi_n = \|n\bar{x} + \phi\mu\|_2, \quad \mu_n = (n\bar{x} + \phi\mu)/\phi_n$$

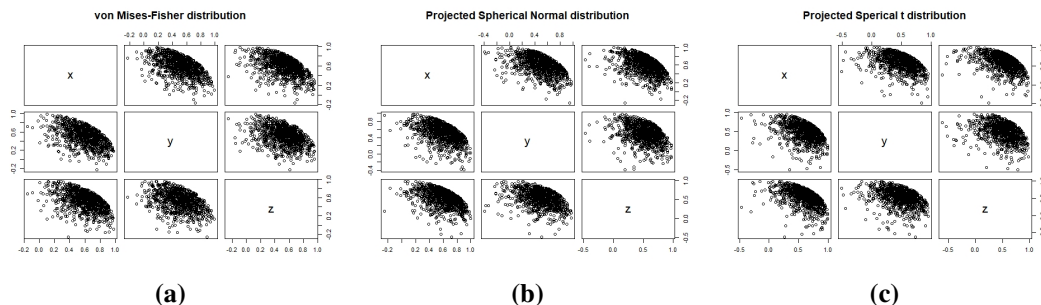


Fig. 3: Pairs plot of 1000 random samples from different constrained posterior distributions on a unit sphere on \mathbb{R}^3 . Data are generated from a Gaussian $N(\theta, 10I)$ with $\theta = [1/\sqrt{3}, 1/\sqrt{3}, 1/\sqrt{3}]$. The samples are drawn from the posterior with (a) the prior distribution $\text{VMF}(\mu, 0.1I_3)$, projecting onto unit sphere after sampling with the prior distribution (b) $N(\mu, 0.1I_3)$, (c) $t_3(\mu, 0.1I_3)$ where $\mu = \theta$.

Alternatively, one can leverage our projection approach by using an unconstrained Gaussian prior $N(\mu, \phi^{-1}I)$ on θ and projecting the posterior samples onto $\tilde{\Theta}$ via the Euclidean norm. Additionally, projection makes it easy to consider different unconstrained prior distributions, such as t-densities to allow heavier tails. Figure 3 demonstrates posterior samples using von Mises-Fisher, projected spherical normal and projected spherical t distributions.

5. EXPERIMENTS

5.1. Stochastic ordering on a contingency table

Data in the form of a contingency table arise when individuals are classified according to multiple criterion. Often, one or more of the categorical variables have a natural ordering, such as in dose-response studies with the ordered levels corresponding to increasing levels of exposure. Methods that take into account the orderings among categories of classifications benefit in terms of more accurate parameter estimation and better power in hypothesis testing. Agresti & Coull (2002) survey order-restricted statistical methods for contingency tables where these restrictions translate to inequality constraints for a set of probabilities, odds ratios or model parameters. We demonstrate the applicability of our posterior projection method with stochastic ordering constraints and discuss how other constraints can be incorporated.

For simplicity we consider a two way $I \times J$ contingency table with cell entries n_{ij} , $i = (1, \dots, I)$, $j = (1, \dots, J)$ and $\sum_{i=1}^I \sum_{j=1}^J n_{ij} = n$. The rows and columns denote the categories of predictor variable X and response variable Y , respectively. We assume that the rows of the contingency table are independent multinomial samples from different populations with sample sizes $n_{i+} = \sum_{j=1}^J n_{ij}$ and probability vector $\theta_{(i)} = (\theta_{i1}, \dots, \theta_{iJ})$. Under this setup the condition of Y being stochastically increasing in X translates to

$$\sum_{k=1}^j \theta_{ik} \geq \sum_{k=1}^j \theta_{(i+1),k} \quad i = (1, \dots, I), j = (1, \dots, J). \quad (13)$$

Laudy & Hoijtink (2007) use gamma parametrization of Dirichlet to put a truncated prior on $\theta = (\theta'_{(1)}, \dots, \theta'_{(I)})$ which follows the restriction in (13). This method is attractive as it allows one to sample from a Dirichlet-multinomial model under a variety of odds ratio constraints. However their sampling

technique, which uses the odds ratio inequalities to truncate the gamma prior for every individual parameter at every Gibbs sampling update, is computationally expensive and relatively slow. To circumvent this difficulty we initially ignore the constraint and assign a conjugate Dirichlet prior on $\theta_{(i)}$ with equal hyperparameter α for all the components. The unconstrained posterior distribution of $\theta_{(i)}$ is given by

$$\theta_{(i)} \sim \text{Dir}(n_{i1} + \alpha, \dots, n_{iJ} + \alpha). \tag{14}$$

We observe that equation (13) along with $\sum_{j=1}^J \theta_{ij} = 1$ induces linear inequality and equality restrictions on θ . Thus one can use the pooled adjacency violator algorithm Barlow (1972) to find the $\tilde{\theta}$ that minimizes a convex functional of θ under the stochastic order and probability restrictions. We choose Euclidean distance as the convex functional in our application, that is $\tilde{\theta}_E$ minimizes

$$\tau^2 = \sum_{i=1}^I \sum_{j=1}^J (\theta_{ij} - \tilde{\theta}_{ij})^2. \tag{15}$$

Evans et al. (1997) uses the sampled values of τ^2 to construct a test for the hypothesis $H_t = \{\theta \mid \tau(\theta)^2 \leq t^{0.5}\}$ against the alternative H_t^c , under stochastic ordering constraint.

We consider the data from Agresti & Coull (1998) which describes the outcome of a sample of patients with a trauma due to subarachnoid Hemorrhage. Patients are divided into four treatment groups. The first group receives a placebo and the rest of the groups are administered increasing doses of a medicine. The outcome of the clinical study is sorted into 5 categories according to the Glasgow Outcome Scale. An interesting way to see if the data exhibits stochastic ordering is to consider the difference of the sampled and projected probabilities under prior and posterior measures. To this end we draw 10000 samples from both the prior and the posterior, calculate the projection and plot the empirical distribution function of τ^2 (15). Figure 4 shows that the τ^2 value is much smaller in general under the posterior which is an indication of the data following stochastic order.

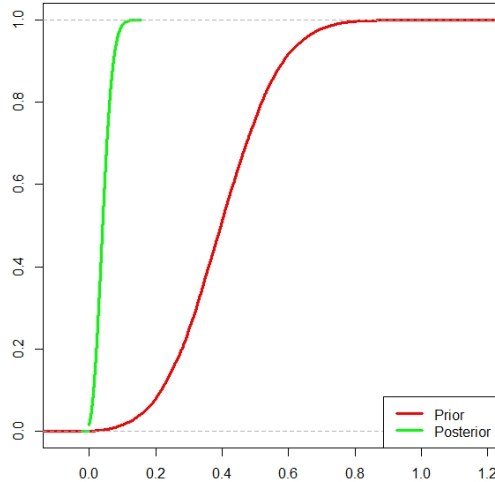


Fig. 4: Empirical cumulative distribution function of τ^2 under prior and posterior measure with $\alpha = 1$

Encouraged by this evidence of the constraint, we apply our projection method to the data. After some experimentation the value of α in the posterior (14) is fixed at 1. We draw 10000 samples from the posterior and compute the corresponding projections. The projected probabilities along with credible intervals

are provided in the Supplementary Materials. We also compare the effect of the projection by comparing the cumulative odds ratios in Table 1 and observe that without projection the estimated value of the odds ratio is sometimes less than 1. This is in contradiction to our assumption as when the rows of the categorical table are assumed to be independent Multinomials, the stochastic ordering constraint is equivalent to the cumulative odds ratio being uniformly greater than 1. We also take note that our method produces tighter credible intervals than Laudy & Hoijtink (2007).

	1-2	2-3	3-4	4-5
1-2	1.147 (1.000 – 1.477)	1.132 (1.000 – 1.372)	1.060 (1.000 – 1.193)	1.014 (1.000 – 1.070)
	1.128 (0.807 – 1.546)	1.108 (0.858 – 1.400)	1.043 (0.889 – 1.215)	1.007 (0.925 – 1.096)
2-3	1.160 (1.000 – 1.511)	1.291 (1.037 – 1.618)	1.109 (1.000 – 1.261)	1.007 (1.000 – 1.057)
	1.207 (0.833 – 1.705)	1.302 (0.970 – 1.716)	1.101 (0.928 – 1.297)	0.992 (0.911 – 1.080)
3-4	1.055 (1.000 – 1.365)	1.219 (1.003 – 1.570)	1.107 (1.000 – 1.299)	1.067 (1.000 – 1.158)
	0.983 (0.667 – 1.417)	1.175 (0.839 – 1.619)	1.100 (0.908 – 1.322)	1.075 (0.980 – 1.178)

Table 1: Estimates and credible intervals of cumulative odds ratio under the Dirichlet-multinomial model with $\alpha = 1$. Within each row the upper and lower row contains results using the projection method and sampling from the posterior disregarding the stochastic ordering constraint, respectively. The bold numbers indicate where stochastic ordering fails without projection.

We also investigate the effect of the value of the hyperparameter α . As α increases, more mass is put onto the convex set of probabilities following stochastic order and hence the mean of τ^2 decreases. The posterior mean of τ^2 is unaffected by the change.

Value of α	0.1	0.5	1	5	10
Prior mean of τ^2	0.795	0.525	0.402	0.192	0.138
Posterior mean of τ^2	0.043	0.042	0.042	0.040	0.039

Table 2: Sensitivity analysis of hyperparameter α on τ^2 .

We briefly discuss how our method can be applied to other scenarios.

Norm and hyperplane restrictions: Two important examples of norm restrictions on parameters are ridge regression and lasso regression, which fits a linear regression model under the restriction that $\|\beta\|_2 \leq \lambda$ and $\|\beta\|_1 \leq \lambda$ respectively, for some constant $\lambda > 0$. The norm-0 restriction $\|\beta\|_0 \leq \lambda$ has also gained popularity as an effective sparsity inducing method; see (Fu, 1998) for a detailed discussion on these methods. A linear equality or inequality constraint such as lasso is equivalent to specifying a hyperplane whereas a quadratic restriction such as ridge requires a spherical projection. Many such norm regularization and penalty constraints, like elastic net (Zou & Hastie, 2005), are equivalent to simple projection onto closed convex sets. Therefore our method can be applied by choosing suitable conjugate priors and appropriate efficient algorithms for projection. The posterior projection framework has potential advantages in terms of uncertainty quantification and use of a Bayesian approach for tuning parameter choice avoiding cross validation.

5.2. Analyzing brain network

An emerging paradigm in neuroscience is that any cognitive task is performed by several brain regions which are anatomically separate but functionally linked. The study of the physical and functional con-

nections between different brain regions, called the “connectome” is facilitated by modern noninvasive imaging techniques. We analyze the DTI sequence data from the KKI-42 (Landman et al., 2011) dataset, consisting of two scans for $N = 21$ volunteers without any prior history of neuropsychiatric diseases. We use the first scan to estimate model parameters and validate the model on the second scan. Recent connectome preprocessing pipelines (Craddock et al., 2013) were used on the DTI imaging to produce an $m \times m$ symmetric adjacency matrix X_n for every individual $n = 1, \dots, N$. In our application $m = 68$ and a particular node $i = 1, \dots, m$ characterizes a specific brain region according to the Desikan et al. (2006) atlas. $X_{nij} \in \{0, 1\}$ is an indicator of a white fiber connection between brain regions $i = 2, \dots, m$ and $j = 1, \dots, i - 1$ for the n th individual. $X_{nii} = 0$ for all $i = 1, \dots, m$ and we use only the lower triangular part due to symmetry.

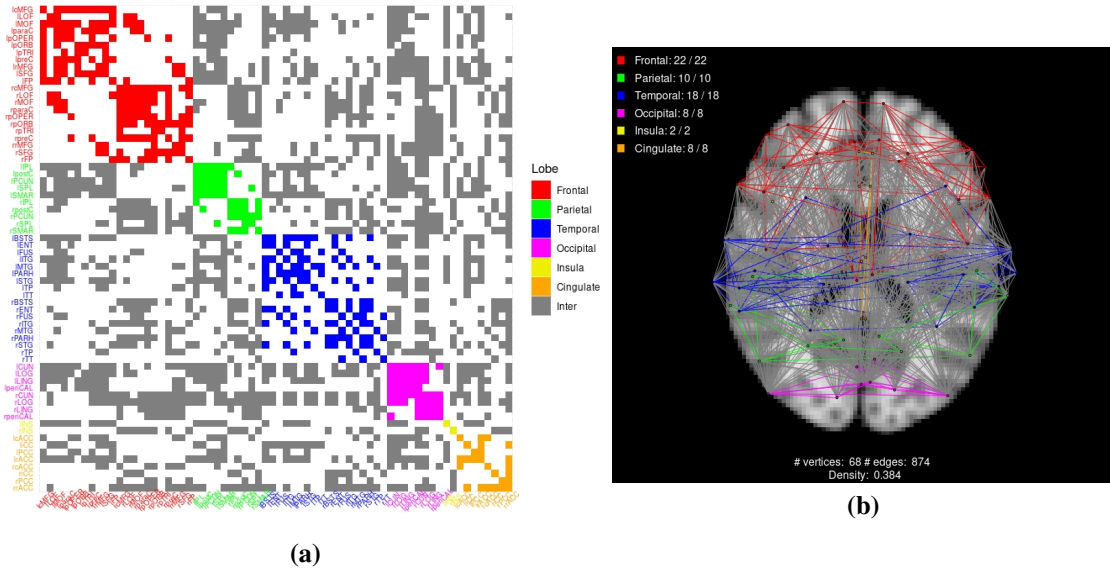


Fig. 5: Illustration of a sample of the data displaying (a) adjacency matrix and (b) brain network obtained from the first scan of the first volunteer. The brain regions and the associated lobe membership are chosen according to the Desikan atlas. Both the plots were generated by the BrainGraph package in R.

Following Hoff (2008) we model the brain network as the following reduced-rank logit model:

$$X_{nij} \sim \text{Bern}(\pi_{nij}), \quad \log\left(\frac{\pi_{nij}}{1 - \pi_{nij}}\right) = Z_{ij} + u_i^T \Lambda_n u_j, \quad (16)$$

where $\Lambda_n = \text{diag}(\Lambda_{n1}, \dots, \Lambda_{np})$ and u_i are p -dimensional column vectors. We choose $p = 10$ as an upper bound on the number of subnetworks consistent with our discussion in section 4.1. The probability of a link between node i and j in the connectivity graph for the n th individual depends on their similarity in a space of unobserved latent characteristics. The latent factor $\Lambda_{nk}, k = (1, \dots, p)$ is a person specific effect on brain subnetwork k and u_{ik} represents the effect of brain region i on subnetwork k . Z_{ij} is the baseline log-odds of a connection between the (i, j) pair of brain regions. The singular value decomposition like representation of the dataset in equation (16) naturally suggests a constraint of orthonormality on u_i . This restriction is necessary for the model to be identifiable which is important for interpretation purposes (Hoff, 2016). We remove rotational and scaling ambiguity by assuming that the matrix U with row vectors u_1, \dots, u_m lies on the Stiefel manifold $\text{St}(p, m) = \{U : U^T U = I_p\}$. Instead of enforcing this sharp constraint, Duan et al. (arXiv:1801.01525v2) considers a constraint relaxed model on the data and therefore does not have exact orthogonality on U .

On average we found only 36% of the brain regions to be connected across all the subjects in the dataset, a significant portion of which are intra-lobe connections. Because of the relatively low number of connections, it is reasonable to assume only a few brain regions will contribute to a particular subnetwork. Therefore, we induce sparsity on the brain subnetworks, parameterised by the factor matrix U , through shrinkage priors. However, the well known matrix Bingham-von Mises–Fisher (BMF) family of priors on $\text{St}(p, m)$ does not induce much shrinkage. Therefore, we take advantage of our method by initially ignoring the Stiefel manifold restriction and putting independent Dirichlet-Laplace (DL) shrinkage priors on the columns of U (Bhattacharya et al., 2015). The hyperparameters for the inverse gamma are chosen so that the priors are weakly informative. As advised in the source literature, the value of the parameter a in the DL prior was fixed at $1/2$ and $1/m$ in two different runs of the model.

$$\begin{aligned} Z_{ij} &\sim \text{N}(0, \sigma_Z^2), & \Lambda_{nk} &\sim \text{N}(0, \sigma_k^2), & u_k &\sim \text{DL}_a \\ \sigma_Z^2 &\sim \text{IG}(2, 1), & \sigma_k^2 &\sim \text{IG}(2, 1), & k &= (1, \dots, p) \end{aligned} \quad (17)$$

The model was fit in RStan using the No U-Turn Sampler algorithm. We discarded the first 5000 draws of 10000 iterations as burn-in. The convergence and mixing rates of the sampler were adequate. To remove scaling ambiguity, posterior samples of U were normalized to the unit spectral ball prior to projection. These norm values were absorbed in the factor loading matrix Λ to obtain $U_l^{(s)} = U^{(s)} / \|U^{(s)}\|_2$ and $(\Lambda_n)_l^{(s)} = \Lambda_n^{(s)} * \|U^{(s)}\|_2^2$, respectively. These $U_l^{(s)}$ samples are then projected onto the Stiefel manifold and multiplied by $\|U^{(s)}\|$ to get $\tilde{U}^{(s)}$. In the event $U_l^{(s)}$ does not have a unique projection we choose any one of its projections as per our discussion in Lemma 4. The projection routine was implemented using the Manopt package from Matlab (Nicolas et al., 2014). The projection estimate for the logit function of π_{nij} from the s th sample is given by $Z_{ij}^{(s)} + \tilde{u}_i^{(s)T} (\Lambda_n)_i^{(s)} \tilde{u}_j^{(s)}$.

The brightly colored regions along the diagonal in Fig. 5(a) represent the intra-lobe connections. Brain regions within a single lobe, represented by a particular color, are spatially close and therefore are generally connected among most subjects. These, along with some frequent inter-lobe connections, are accounted for by the Z matrix in (16). The role of the factor matrix U is to reveal the more obscure relationship present in the data beyond the spatial association. With strong shrinkage our method clearly detects subnetwork membership as opposed to the unrestricted method (Fig. 6). In the absence of the orthogonality constraint the posterior sample means of the elements of the factor matrix u_{ik} are scattered around 0. The projection technique maps the very small values to 0 while inflating others, bringing out the subnetwork structure. The differences in the results is depicted in Fig. 6.

The prominent subnetwork structure in the factor matrix of the projection method allows us to interpret the connectomes that are not spatially associated. As an example, the 3rd factor under the projected model puts brain regions Superior Parietal, Pars Orbitalis, Pericalcarine and Lateral Occipital Gyrus in the same subnetwork. These brain regions have been associated with spatial orientation, visual and sensory input from hands, processing of syntax in the oral and sign language, musical syntax, primary visual cortex (Coullon et al., 2015) and face perception (Nagy et al., 2012) and hence form a sensible subnetwork. With $\text{DL}_{1/2}$ prior the projection still retains its utility by forcing small values of u_{ik} towards 0, but it fails to indicate any strong membership.

Prior	$\text{DL}_{1/m}$		$\text{DL}_{1/2}$	
	Unrestricted	Projected	Unrestricted	Projected
Fitted AUC	96.8	93.8	98.8	88.2
Prediction AUC	95.8	91.3	95.0	86.1

Table 3: Estimation and cross validation area under the curve (AUC) measure for the KKI-42 dataset under different Dirichlet–Laplace priors.

One can build a classifier algorithm based on the posterior probabilities π_{nij} by estimating X_{nij} to be 1 above a threshold value and 0 otherwise. We validate our model by testing the accuracy of this binary

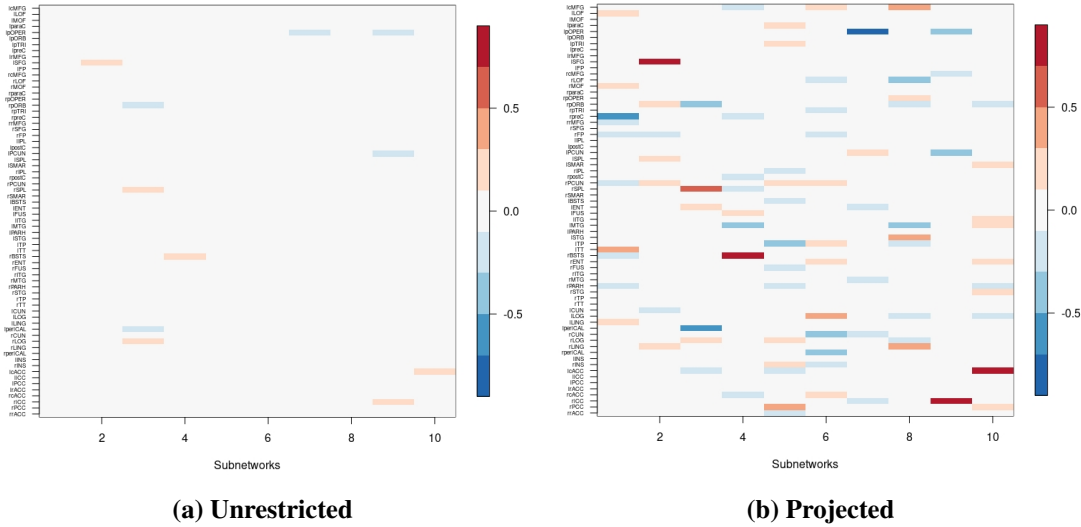


Fig. 6: Posterior sample mean of the factor matrix U (a) before projection and (b) after projection under $DL_{1/m}$ prior. The columns are sorted according to decreasing value of σ_k^2 . The rows are rearranged to match Desikan atlas as in Fig. 5.

classifier against the held out second scan. As the results depend on the chosen cutoff level, we estimate the receiver operating characteristic curves (ROC) and compare methods based on area under the curve (AUC). With strong shrinkage the projected model has similar predictive performance as the unrestricted model, but falls of substantially otherwise (Table 3). This is expected as the projection method is designed to enhance interpretability through constraints, and such interpretability may have a cost.

6. SUMMARY & FUTURE RESEARCH

This article has developed the fundamental underpinning for a general new approach for constrained Bayesian inference. There are many interesting new directions. One important generalization is to allow conditional posterior projections; for example, applying projection to a subset of parameters immediately after each update step within a Markov chain Monte Carlo algorithm. Another direction is studying when projected posteriors are expected to produce better results than traditional approaches; for example, obtaining lower risk parameter estimates. Also of considerable interest is the construction of formal goodness-of-fit test of the constraint, as well as adaptive procedures that avoid projecting when the cost to goodness-of-fit is too high.

7. ACKNOWLEDGEMENTS

We would like to thank Surya T. Tokdar and Robert L. Wolpert for their insightful discussions that have led to an improved presentation, and some corrections. We would also like to thank Rebecca C. Steerts for commenting on our work and giving helpful suggestions that have improved the writing.

REFERENCES

ABSIL, P.-A. & MALICK, J. (2012). Projection-like retractions on matrix manifolds. *SIAM Journal on Optimization* **22**, 135–158.

- AGGARWAL, G., CHOWDHURY, A. R. & CHELLAPPA, R. (2004). A system identification approach for video-based face recognition. In *Pattern Recognition, 2004. ICPR 2004. Proceedings of the 17th International Conference on*, vol. 4. IEEE.
- AGRESTI, A. & COULL, B. A. (1998). Order-restricted inference for monotone trend alternatives in contingency tables. *Computational Statistics & Data Analysis* **28**, 139–155.
- AGRESTI, A. & COULL, B. A. (2002). The analysis of contingency tables under inequality constraints. *Journal of Statistical Planning and Inference* **107**, 45–73.
- BARDELLI, E. & MENNUCCI, A. C. G. (2017). Probability measures on infinite-dimensional stiefel manifolds. *Journal of Geometric Mechanics* **9**, 291–316.
- BARLOW, R. E. (1972). *Statistical Inference Under Order Restrictions: The Theory and Application of Isotonic Regression*. Chichester : Wiley.
- BHATTACHARYA, A., PATI, D., PILLAI, N. S. & DUNSON, D. B. (2015). Dirichlet-laplace priors for optimal shrinkage. *Journal of the American Statistical Association* **110**, 1479–1490.
- COULLON, G. S., EMIR, U. E., FINE, I., WATKINS, K. E. & BRIDGE, H. (2015). Neurochemical changes in the pericalcarine cortex in congenital blindness attributable to bilateral anophthalmia. *J Neurophysiol* **114**, 1725–33.
- CRADDOCK, R. C., JBABDI, S., YAN, C.-G., VOGELSTEIN, J. T., CASTELLANOS, F. X., DI MARTINO, A., KELLY, C., HEBERLEIN, K., COLCOMBE, S. & MILHAM, M. P. (2013). Imaging human connectomes at the macroscale. *Nature Methods* **10**, 524.
- DESIKAN, R. S., SEGONNE, F., FISCHL, B., QUINN, B. T., DICKERSON, B. C., BLACKER, D., BUCKNER, R. L., DALE, A. M., MAGUIRE, R. P., HYMAN, B. T., ALBERT, M. S. & KILLIANY, R. J. (2006). An automated labeling system for subdividing the human cerebral cortex on mri scans into gyral based regions of interest. *Neuroimage* **31**, 968–80.
- DUNSON, D. B. & NEELON, B. (2003). Bayesian inference on order-constrained parameters in generalized linear models. *Biometrics* **59**, 286–295.
- EDELMAN, A., ARIAS, T. A. & SMITH, S. T. (1998). The geometry of algorithms with orthogonality constraints. *SIAM journal on Matrix Analysis and Applications* **20**, 303–353.
- EVANS, M., GILULA, Z., GUTTMAN, I. & SWARTZ, T. (1997). Bayesian analysis of stochastically ordered distributions of categorical variables. *Journal of the American Statistical Association* **92**, 208–214.
- FITZPATRICK, S. & PHELPS, R. R. (1982). Differentiability of the metric projection in hilbert space. *Transactions of the American Mathematical Society* **270**, 483–501.
- FU, W. J. (1998). Penalized regressions: the bridge versus the lasso. *Journal of computational and graphical statistics* **7**, 397–416.
- GHOSAL, S. & VAN DER VAART, A. (2017). *Fundamentals of Nonparametric Bayesian Inference*, vol. 44. Cambridge University Press.
- GOODALL, C. R. & MARDIA, K. V. (1999). Projective shape analysis. *Journal of Computational and Graphical Statistics* **8**, 143–168.
- GUNN, L. H. & DUNSON, D. B. (2005). A transformation approach for incorporating monotone or unimodal constraints. *Biostatistics* **6**, 434–449.
- HOFF, P. (2008). Modeling homophily and stochastic equivalence in symmetric relational data. In *Advances in Neural Information Processing Systems 20*, J. Platt, D. Koller, Y. Singer & S. Roweis, eds. Cambridge, MA: MIT Press, pp. 657–664.
- HOFF, P. D. (2016). Equivariant and scale-free tucker decomposition models. *Bayesian Anal.* **11**, 627–648.
- HOROWITZ, J. L. & LEE, S. (2017). Nonparametric estimation and inference under shape restrictions. *Journal of Econometrics* **201**, 108–126.
- JIDLING, C., WAHLSTRM, N., WILLS, A. & SCHN, T. B. (2017). Linearly constrained gaussian processes. In *Advances in Neural Information Processing Systems*.
- JOURNE, M., NESTEROV, Y., RICHTRIK, P. & SEPULCHRE, R. (2010). Generalized power method for sparse principal component analysis. *Journal of Machine Learning Research* **11**, 517–553.
- LANDMAN, B. A., HUANG, A. J., GIFFORD, A., VIKRAM, D. S., LIM, I. A. L., FARRELL, J. A. D., BOGOVIC, J. A., HUA, J., CHEN, M., JARSO, S., SMITH, S. A., JOEL, S., MORI, S., PEKAR, J. J., BARKER, P. B., PRINCE, J. L. & VAN ZIJL, P. C. M. (2011). Multi-parametric neuroimaging reproducibility: A 3t resource study. *NeuroImage* **54**, 2854–2866.
- LAUDY, O. & HOIJTINK, H. (2007). Bayesian methods for the analysis of inequality constrained contingency tables. *Stat Methods Med Res* **16**, 123–38.
- LI, J. (2004). The metric projection and its applications to solving variational inequalities in banach spaces. *Fixed Point Theory* **5**, 285–298.
- LIN, L. & DUNSON, D. B. (2014). Bayesian monotone regression using gaussian process projection. *Biometrika* **101**, 303–317. 10.1093/biomet/ast063.
- NAGY, K., GREENLEE, M. W. & KOVCS, G. (2012). The lateral occipital cortex in the face perception network: An effective connectivity study. *Frontiers in Psychology* **3**, 141.
- NICOLAS, B., BAMDEV, M., ABSIL, P.-A. & RODOLPHE, S. (2014). Manopt, a matlab toolbox for optimization on manifolds. *Journal of Machine Learning Research* **15**, 1455–1459.

- SAARELA, O. & ARJAS, E. (2011). A method for bayesian monotonic multiple regression. *Scandinavian Journal of Statistics* **38**, 499–513.
- SHIVELY, T. S., WALKER, S. G. & DAMIEN, P. (2011). Nonparametric function estimation subject to monotonicity, convexity and other shape constraints. *Journal of Econometrics* **161**, 166–181.
- VEERARAGHAVAN, A., ROY-CHOWDHURY, A. K. & CHELLAPPA, R. (2005). Matching shape sequences in video with applications in human movement analysis. *IEEE Transactions on Pattern Analysis and Machine Intelligence* **27**, 1896–1909.
- ZOU, H. & HASTIE, T. (2005). Regularization and variable selection via the elastic net. *Journal of the Royal Statistical Society: Series B (Statistical Methodology)* **67**, 301–320.

8. SUPPLEMENTARY MATERIAL

Supplementary material includes proofs of the theoretical results in the main paper, detailed calculations and additional tables and examples related to the experiments.

8.1. Existence of prior on constrained parameter space

Proof of Lemma 1. Let $B \in \mathcal{B}_{\tilde{\Theta}}$ such that $\tilde{\mu}_{\tilde{\Theta}}(B) = 0$. Then

$$\tilde{\mu}_{\tilde{\Theta}}(B) = 0 \implies \mu_{\Theta}(T^{-1}B) = 0 \implies \lambda_{\Theta}(T^{-1}B) = 0 \implies \tilde{\lambda}_{\tilde{\Theta}}(B) = 0.$$

This implies $\tilde{\lambda}_{\tilde{\Theta}} \ll \tilde{\mu}_{\tilde{\Theta}}$. □

Proof of Theorem 1. We want a prior density $\pi_{\tilde{\Theta}}(\tilde{\theta})$ on $\tilde{\Theta}$ such that the corresponding posterior is equal to the projected posterior density $\tilde{\pi}_{\tilde{\Theta}}(\tilde{\theta}|X^{(n)})$, that is we want the following to hold.

$$\begin{aligned} \tilde{\pi}_{\tilde{\Theta}}(\tilde{\theta}|X^{(n)}) &= p_{\tilde{\theta}}(X^{(n)}) \pi_{\tilde{\Theta}}(\tilde{\theta}) \left(\int_{\tilde{\Theta}} p_{\tilde{\theta}}(X^{(n)}) \pi_{\tilde{\Theta}}(\tilde{\theta}) d\mu_{\tilde{\Theta}}(\tilde{\theta}) \right)^{-1} \\ \implies \tilde{\pi}_{\tilde{\Theta}}(\tilde{\theta}|X^{(n)}) &\left(\int_{\tilde{\Theta}} p_{\tilde{\theta}}(X^{(n)}) \pi_{\tilde{\Theta}}(\tilde{\theta}) d\mu_{\tilde{\Theta}}(\tilde{\theta}) \right) = p_{\tilde{\theta}}(X^{(n)}) \pi_{\tilde{\Theta}}(\tilde{\theta}). \end{aligned} \quad (\text{S1})$$

We choose $\pi_{\tilde{\Theta}}(\tilde{\theta}) = p_{\tilde{\theta}}(X^{(n)})^{-1} \tilde{\pi}_{\tilde{\Theta}}(\tilde{\theta}|X^{(n)}) \left(\int_{\tilde{\Theta}} p_{\tilde{\theta}}(X^{(n)})^{-1} \tilde{\pi}_{\tilde{\Theta}}(\tilde{\theta}|X^{(n)}) d\mu_{\tilde{\Theta}}(\tilde{\theta}) \right)^{-1}$ which is well defined because of Assumption 1. This also defines a density on $\tilde{\Theta}$ as $\int_{\tilde{\Theta}} \pi_{\tilde{\Theta}}(\tilde{\theta}) d\mu_{\tilde{\Theta}}(\tilde{\theta}) = 1$. Substituting our chosen $\pi_{\tilde{\Theta}}(\tilde{\theta})$ in the left hand side of (S1) we get

$$\begin{aligned} &\tilde{\pi}_{\tilde{\Theta}}(\tilde{\theta}|X^{(n)}) \left[\int_{\tilde{\Theta}} \tilde{\pi}_{\tilde{\Theta}}(\tilde{\theta}|X^{(n)}) \left\{ \int_{\tilde{\Theta}} p_{\tilde{\theta}}(X^{(n)})^{-1} \tilde{\pi}_{\tilde{\Theta}}(\tilde{\theta}|X^{(n)}) d\mu_{\tilde{\Theta}}(\tilde{\theta}) \right\}^{-1} d\mu_{\tilde{\Theta}}(\tilde{\theta}) \right] \\ &= \tilde{\pi}_{\tilde{\Theta}}(\tilde{\theta}|X^{(n)}) \left(\int_{\tilde{\Theta}} \tilde{\pi}_{\tilde{\Theta}}(\tilde{\theta}|X^{(n)}) d\mu_{\tilde{\Theta}}(\tilde{\theta}) \right) \left\{ \int_{\tilde{\Theta}} p_{\tilde{\theta}}(X^{(n)})^{-1} \tilde{\pi}_{\tilde{\Theta}}(\tilde{\theta}|X^{(n)}) d\mu_{\tilde{\Theta}}(\tilde{\theta}) \right\}^{-1} \\ &= \tilde{\pi}_{\tilde{\Theta}}(\tilde{\theta}|X^{(n)}) \left\{ \int_{\tilde{\Theta}} p_{\tilde{\theta}}(X^{(n)})^{-1} \tilde{\pi}_{\tilde{\Theta}}(\tilde{\theta}|X^{(n)}) d\mu_{\tilde{\Theta}}(\tilde{\theta}) \right\}^{-1} \\ &= p_{\tilde{\theta}}(X^{(n)}) \pi_{\tilde{\Theta}}(\tilde{\theta}). \end{aligned}$$

8.2. Posterior convergence of projection method

We study the rate at which the posterior concentrates on arbitrary small neighbourhoods of $P_{\theta_0}^{(n)}$, where $\theta_0 \in \Theta$ denotes the true value of the parameter. Let the unrestricted posterior $\Pi_{\Theta}^{(n)}(\cdot | X^{(n)})$ have rate ϵ_n with respect to a semimetric d_{Θ} on Θ in the following sense:

$$\Pi_{\Theta}^{(n)}\left(\theta : d_{\Theta}(\theta, \theta_0) > M_n \epsilon_n \mid X^{(n)}\right) \rightarrow 0, \quad \text{for every } M_n \rightarrow \infty, \quad P_{\theta_0}^{(n)}(a.s.). \quad (\text{S2})$$

Proof of Theorem 2. From Assumptions 2–4 we can deduce the following inequality. For every $\theta \in \Theta$ and $\tilde{\theta} \in \tilde{\Theta}$,

$$C^{-2}d_{\Theta}(T\theta, \tilde{\theta}) \leq C^{-1}\|T\theta - \tilde{\theta}\| \leq C^{-1}\|\theta - \tilde{\theta}\| \leq d_{\Theta}(\theta, \tilde{\theta}). \quad (\text{S3})$$

Hence, for every $M_n \rightarrow \infty$, $\epsilon_n > 0$ and $\theta_0 \in \tilde{\Theta}$, we have

$$T^{-1} \left\{ \tilde{\theta} : d_{\Theta}(\tilde{\theta}, \theta_0) \geq C^2 M_n \epsilon_n \right\} = \left\{ \theta : d_{\Theta}(T\theta, \theta_0) \geq C^2 M_n \epsilon_n \right\} \subseteq \left\{ \theta : d_{\Theta}(\theta, \theta_0) \geq M_n \epsilon_n \right\}$$

Therefore,

$$\begin{aligned} & \tilde{\Pi}_{\tilde{\Theta}}^{(n)} \left\{ \tilde{\theta} : d_{\Theta}(\tilde{\theta}, \theta_0) > C^2 M_n \epsilon_n \mid X^{(n)} \right\} \\ &= \Pi_{\Theta}^{(n)} \left[T^{-1} \left\{ \tilde{\theta} : d_{\Theta}(\tilde{\theta}, \theta_0) > C^2 M_n \epsilon_n \right\} \mid X^{(n)} \right] \\ &= \Pi_{\Theta}^{(n)} \left\{ \theta : d_{\Theta}(T\theta, \theta_0) > C^2 M_n \epsilon_n \mid X^{(n)} \right\} \\ &\leq \Pi_{\Theta}^{(n)} \left\{ \theta : d_{\Theta}(\theta, \theta_0) > M_n \epsilon_n \mid X^{(n)} \right\} \rightarrow 0 \end{aligned}$$

Because C is a fixed constant the projected posterior converges to θ_0 and has concentration rate at least that of the original posterior. \square

Proof of Corollary 1. All these spaces are separable, uniformly convex and uniformly smooth Banach spaces. \square

Metric projection onto a closed convex subset of Hilbert space is non expansive, that is

$$\|T\theta - T\theta'\| \leq \|\theta - \theta'\|, \quad \text{for any } \theta, \theta' \in \Theta. \quad (\text{S4})$$

Therefore in Hilbert spaces we do not need to assume that $\theta \in \tilde{\Theta}$ and we achieve the following theorem.

Proof of Theorem 3. A similar argument as in the proof of Theorem 3 gives us the following relation. This is similar to equation (S3) in nature, but appropriated to Hilbert space using the non-expansive property (S4). For any $\theta, \theta' \in \Theta$,

$$C^{-2}d_{\Theta}(T\theta, T\theta') \leq C^{-1}\|T\theta - T\theta'\| \leq C^{-1}\|\theta - \theta'\| \leq d_{\Theta}(\theta, \theta').$$

Hence, for every $M_n \rightarrow \infty$, $\epsilon_n > 0$ and $\theta, \theta_0 \in \Theta$, we have

$$T^{-1} \left\{ \theta : d_{\Theta}(\theta, T\theta_0) \geq C^2 M_n \epsilon_n \right\} = \left\{ \theta : d_{\Theta}(T\theta, T\theta_0) \geq C^2 M_n \epsilon_n \right\} \subseteq \left\{ \theta : d_{\Theta}(\theta, \theta_0) \geq M_n \epsilon_n \right\}$$

Therefore,

$$\begin{aligned} & \tilde{\Pi}_{\Theta}^{(n)} \left\{ \theta : d_{\Theta}(\theta, T\theta_0) > C^2 M_n \epsilon_n \mid X^{(n)} \right\} \\ &= \Pi_{\Theta}^{(n)} \left[T^{-1} \left\{ \theta : d_{\Theta}(\theta, T\theta_0) > C^2 M_n \epsilon_n \right\} \mid X^{(n)} \right] \\ &= \Pi_{\Theta}^{(n)} \left\{ \theta : d_{\Theta}(T\theta, T\theta_0) > C^2 M_n \epsilon_n \mid X^{(n)} \right\} \\ &\leq \Pi_{\Theta}^{(n)} \left\{ \theta : d_{\Theta}(\theta, \theta_0) > M_n \epsilon_n \mid X^{(n)} \right\} \rightarrow 0 \end{aligned}$$

Because C is a fixed constant the projected posterior converges to $T\theta_0$ and has concentration rate at least that of the original posterior. \square

Proof of Corollary 2. All these spaces are separable Hilbert spaces. \square

8.3. Generalization of projection of conjugate Gaussian likelihood-prior

As a generalization of the illustrative example we consider projection of a univariate non-standard Gaussian likelihood with conjugate prior onto the closed interval $[c, d]$ on the real line where c and d can be $-\infty$ and ∞ , respectively. Let $X^{(n)} = (x_1, x_2, \dots, x_n)$ be such that $x_i \sim N(\theta, \sigma^2)$, $i = (1, \dots, n)$. When the constrained parameter space is a closed interval on the real line it is common to put a truncated prior on the parameter, that is $\theta \sim N_{(c,d)}(\theta_0, \sigma_0^2)$. Here $N_{(c,d)}$ denotes the normal distribution truncated between c and d . The posterior of θ is then given by

$$\theta | X^{(n)}, \sigma^2 \sim N_{(c,d)}(\theta_n, \sigma_n^2), \quad \theta_n = \sigma_n^2 (\theta_0/\sigma_0^2 + n\bar{x}/\sigma^2), \quad \sigma_n^2 = (1/\sigma_0^2 + n/\sigma^2)^{-1}. \quad (S5)$$

This is equivalent to sampling from the unconstrained posterior and discarding values outside c and d . This posterior density assigns 0 probability to the boundaries and has expectation

$$E(\theta | X^{(n)}, \sigma^2) = \theta_n + \frac{\phi(\alpha) - \phi(\beta)}{\Phi(\beta) - \Phi(\alpha)} \sigma_n \quad (S6)$$

where $\alpha = (c - \theta_n)/\sigma_n$, $\beta = (d - \theta_n)/\sigma_n$ and ϕ and Φ respectively denotes the density and distribution function of standard normal.

In the posterior projection approach we initially ignore the constraint on θ , and use the unrestricted prior $\theta \sim N(\theta_0, \sigma_0^2)$. The resulting posterior is $\theta | X^{(n)} \sim N(\theta_n, \sigma_n^2)$ which has the same form as equation (S5) but without the truncation. Let us denote this probability measure by $\Pi_{\mathbb{R}}^{(n)}$. Next we obtain samples θ_s from the unconstrained posterior and set $\tilde{\theta}_s$ to either c , θ_s or d according to whether θ_s is less than c , between c and d , or greater than d , respectively. Thus for any $B \in \mathcal{B}_{[c,d]}$ the projected posterior measure is given by

$$\tilde{\Pi}_{[c,d]}^{(n)}(B) = \Pi_{\mathbb{R}}^{(n)}(-\infty, c) \mathbb{1}_B(c) + \Pi_{\mathbb{R}}^{(n)}((c, d) \cap B) + \Pi_{\mathbb{R}}^{(n)}(d, \infty) \mathbb{1}_B(d) \quad (S7)$$

Here $\mathbb{1}_B(c)$ is 1 if $c \in B$ and 0 otherwise. It is easy to see that this posterior (S7) does not have a density with respect to $\mu_{\mathbb{R}}$, the Lebesgue measure in \mathbb{R} , as it has point mass at c and d . One might think that because the metric projection preserves absolute continuity (Lemma 1), $\tilde{\Pi}_{[c,d]}^{(n)}(\cdot | X^{(n)}, \sigma^2)$ will have a density with respect to the projected Lebesgue measure in $[c, d]$, which is given by

$$\begin{aligned} \tilde{\mu}_{[c,d]}(B) &= \mu_{\mathbb{R}}(-\infty, c) \mathbb{1}_B(c) + \mu_{\mathbb{R}}((c, d) \cap B) + \mu_{\mathbb{R}}(d, \infty) \mathbb{1}_B(d) \\ &= \Phi(\alpha) \mathbb{1}_B(c) + \mu_{\mathbb{R}}((c, d) \cap B) + \Phi(-\beta) \mathbb{1}_B(d). \end{aligned}$$

But $\tilde{\mu}_{[c,d]}$ is not σ -finite as $\tilde{\mu}_{[c,d]}(c) = \infty$, therefore the condition for Radon-Nikodym derivative is not satisfied. However, one can construct a σ -finite reference measure λ by putting point mass $t_c, t_d \in \mathbb{R}$ at c and d .

$$\lambda_{[c,d]}(B) = t_c \mathbb{1}_B(c) + \mu_{\mathbb{R}}((c, d) \cap B) + t_d \mathbb{1}_B(d) \quad (S8)$$

It can be checked that the projected prior measure is a version of the reference measure when the measure in the interior of the set (c, d) is chosen as the prior measure $\Pi_{\mathbb{R}}$ instead of $\mu_{\mathbb{R}}$. If we fix $t_c = t_d = 1$, then the projected posterior on the interval $[c, d]$ has the following density with respect to (S8).

$$\tilde{\pi}_{[c,d]}^{(n)}(\tilde{\theta}) = \Phi(\alpha) \mathbb{1}_c(\tilde{\theta}) + [\Phi(\beta) - \Phi(\alpha)] N_{(c,d)}(\tilde{\theta}; \theta_n, \sigma_n^2) + \Phi(-\beta) \mathbb{1}_d(\tilde{\theta}) \quad (S9)$$

This posterior density (S9) has expectation

$$E(\tilde{\theta} | X^{(n)}, \sigma^2) = c \Phi(\alpha) + [\Phi(\beta) - \Phi(\alpha)] \left(\theta_n + \frac{\phi(\alpha) - \phi(\beta)}{\Phi(\beta) - \Phi(\alpha)} \sigma_n \right) + d \Phi(-\beta).$$

It is also possible to determine the prior on the interval $[c, d]$ which leads to the projected posterior density in (S9). Any such prior density must have point masses at the boundary. Let the density be

$$\pi_{[c,d]}(\tilde{\theta}) = w_1 \mathbb{1}_c(\tilde{\theta}) + w_2 N_{(c,d)}(\tilde{\theta}; \theta_0, \sigma_0^2) + w_3 \mathbb{1}_d(\tilde{\theta})$$

A simple calculation shows that the posterior under the Gaussian likelihood with this prior leads to the following posterior density.

$$\pi_{[c,d]}^{(n)}(\tilde{\theta}) = W_1 \mathbb{1}_c(\tilde{\theta}) + W_2 N_{(c,d)}(\tilde{\theta}; \theta_n, \sigma_n^2) + W_3 \mathbb{1}_d(\tilde{\theta}),$$

where $W_j = \frac{w_j C_j}{\sum_{j=1}^3 w_j C_j}$ for $j \in \{1, 2, 3\}$ and C_j are derived as follows:

$$\begin{aligned} C_1 &= \int_c^d \frac{\sqrt{n}}{\sigma} \phi\left(\frac{\sqrt{n}(\bar{x} - \tilde{\theta})}{\sigma}\right) \mathbb{1}_c(\tilde{\theta}) d\tilde{\theta} = N(c; \bar{x}, \sigma^2/n). \\ C_2 &= \int_c^d \frac{\sqrt{n}}{\sigma} \phi\left(\frac{\sqrt{n}(\bar{x} - \tilde{\theta})}{\sigma}\right) \mathbb{1}_d(\tilde{\theta}) d\tilde{\theta} = N(d; \bar{x}, \sigma^2/n). \\ C_3 &= \int_c^d \frac{\sqrt{n}}{\sigma} \phi\left(\frac{\sqrt{n}(\bar{x} - \tilde{\theta})}{\sigma}\right) N_{(c,d)}(\tilde{\theta}; \theta_n, \sigma_n^2) d\tilde{\theta} = N(\bar{x}; 0, \sigma^2/n) \frac{N_{(c,d)}(0; \theta_0, \sigma_0^2)}{N_{(c,d)}(0; \theta_n, \sigma_n^2)}. \end{aligned}$$

If we denote the weights of the projected posterior density in (S9) as W_j^0 , then our goal is to find w_j such that $W_j = W_j^0$. If one selects $w_j = (W_j^0/C_j)/(\sum_{j=1}^3 W_j^0/C_j)$, then this is satisfied.

8.4. Metric projection onto Stiefel manifold

Proof of Lemma 2. The proof of this proposition is immediate from the statement of the proposition 4.2 of Bardelli & Mennucci (2017) as $\text{St}(p, m)$ is a closed set of the Riemannian manifold $\mathbb{R}^{m \times p}$. A detailed proof can be found in references therein. \square

Proof of Proposition 1. We note a result from linear algebra that states that an element of $\mathbb{R}^{m \times p}$ is in Θ_p if and only if it has a $p \times p$ invertible submatrix. Therefore we define the function $f(\theta) = \sum_B |\det(B)|$ for $\theta \in \mathbb{R}^{m \times p}$ where the sum is over all $p \times p$ submatrices. Clearly f is continuous, so $\Theta_p = f^{-1}(\mathbb{R}^{m \times p} \setminus \{0\})$ is an open set. \square

Proof of Lemma 4. For any $\theta \in \mathbb{R}^{m \times p}$, $\tilde{\theta} \in \text{St}(p, m)$ we have

$$\begin{aligned} \|T\theta - \tilde{\theta}\| &\leq \|T\theta - \theta\| + \|\theta - \tilde{\theta}\|, \quad \text{triangle inequality} \\ &\leq 2\|\theta - \tilde{\theta}\| \quad \text{from definition of } T\theta. \end{aligned}$$

Proof of Theorem 5. We present an argument similar to that of Theorem 3. However we focus on Θ_p , the set of all rank p matrices instead of $\mathbb{R}^{m \times p}$, as we showed in Lemma 2 that Θ_p has probability 1. This is similar to equation (S3) in nature, but characterized for Stiefel manifolds. For any $\theta \in \Theta_p$, $\tilde{\theta} \in \text{St}(p, m)$,

$$\frac{1}{2}C^{-2}d_{\Theta}(T\theta, \tilde{\theta}) \leq \frac{1}{2}C^{-1}\|T\theta - \tilde{\theta}\| \leq C^{-1}\|\theta - \tilde{\theta}\| \leq d_{\Theta}(\theta, \tilde{\theta}).$$

Hence, for every $M_n \rightarrow \infty$, $\epsilon_n > 0$ and $\theta_0 \in \tilde{\Theta} = \text{St}(p, m)$, we have

$$T^{-1} \left\{ \tilde{\theta} : d_{\Theta}(\tilde{\theta}, \theta_0) \geq 2C^2 M_n \epsilon_n \right\} = \left\{ \theta : d_{\Theta}(T\theta, \theta_0) \geq 2C^2 M_n \epsilon_n \right\} \subseteq \left\{ \theta : d_{\Theta}(\theta, \theta_0) \geq M_n \epsilon_n \right\}$$

Therefore,

$$\begin{aligned} &\tilde{\Pi}_{\tilde{\Theta}}^{(n)} \left\{ \tilde{\theta} : d_{\Theta}(\tilde{\theta}, \theta_0) > 2C^2 M_n \epsilon_n \mid X^{(n)} \right\} \\ &= \Pi_{\Theta}^{(n)} \left[T^{-1} \left\{ \tilde{\theta} : d_{\Theta}(\tilde{\theta}, \theta_0) > 2C^2 M_n \epsilon_n \right\} \mid X^{(n)} \right] \\ &= \Pi_{\Theta}^{(n)} \left\{ \theta \in \Theta_p : d_{\Theta}(T\theta, \theta_0) > 2C^2 M_n \epsilon_n \mid X^{(n)} \right\} \\ &\leq \Pi_{\Theta}^{(n)} \left\{ \theta \in \Theta_p : d_{\Theta}(\theta, \theta_0) > M_n \epsilon_n \mid X^{(n)} \right\} \rightarrow 0 \end{aligned}$$

Because C is a fixed constant the projected posterior converges to θ_0 and has concentration rate at least that of the original posterior. \square

8.5. *Stochastic ordering on contingency table*

We model the data from Agresti & Coull (1998) via a Dirichlet-Multinomial model. The unconstrained posterior is given by equation (14) with $\alpha = 1$. We then apply the posterior projection approach to account for the stochastic ordering. The estimated cell probabilities and confidence intervals of the resultant method is provided in table 4.

Treatment group	Outcome				
	Death	Vegetative state	Major disability	Minor disability	Good recovery
Placebo	0.285 (0.236 – 0.342)	0.124 (0.088 – 0.166)	0.221 (0.171 – 0.275)	0.227 (0.178 – 0.278)	0.143 (0.105 – 0.177)
Low dose	0.251 (0.206 – 0.300)	0.113 (0.074 – 0.157)	0.232 (0.179 – 0.288)	0.249 (0.200 – 0.304)	0.155 (0.124 – 0.189)
Medium dose	0.218 (0.178 – 0.258)	0.065 (0.035 – 0.102)	0.256 (0.202 – 0.312)	0.301 (0.245 – 0.359)	0.161 (0.130 – 0.199)
High dose	0.207 (0.165 – 0.248)	0.027 (0.009 – 0.051)	0.252 (0.197 – 0.310)	0.299 (0.242 – 0.362)	0.214 (0.165 – 0.290)

Table 4: Estimates and credible intervals of the cell probability under the projection approach with $\alpha = 1$.